Annu. Rev. Biomed. Eng. 2000. 02:315–37

CURRENT METHODS IN MEDICAL IMAGE SEGMENTATION[1]

Dzung L. Pham[2,3], Chenyang Xu[2], and Jerry L. Prince[2]
[2]Department of Electrical and Computer Engineering, The Johns Hopkins University, Baltimore, Maryland 21218; e-mail: pham@jhu.edu, chenyang@jhu.edu, prince@jhu.edu. [3]Laboratory of Personality and Cognition, National Institute on Aging, Baltimore, Maryland 21224

Key Words medical imaging, image processing, classification, deformable models, magnetic resonance imaging

■ **Abstract** Image segmentation plays a crucial role in many medical-imaging applications, by automating or facilitating the delineation of anatomical structures and other regions of interest. We present a critical appraisal of the current status of semi-automated and automated methods for the segmentation of anatomical medical images. Terminology and important issues in image segmentation are first presented. Current segmentation approaches are then reviewed with an emphasis on the advantages and disadvantages of these methods for medical imaging applications. We conclude with a discussion on the future of image segmentation methods in biomedical research.

CONTENTS

[1]The US Government has the right to retain a nonexclusive, royalty-free license in and to any copyright covering this paper.

INTRODUCTION

Diagnostic imaging is an invaluable tool in medicine. Magnetic resonance imaging (MRI), computed tomography (CT), digital mammography, and other imaging modalities provide an effective means for noninvasively mapping the anatomy of a subject. These technologies have greatly increased knowledge of normal and diseased anatomy for medical research and are a critical component in diagnosis and treatment planning.

The growing size and number of these medical images have necessitated the use of computers to facilitate processing and analysis. In particular, computer algorithms for the delineation of anatomical structures and other regions of interest are becoming increasingly important in assisting and automating specific radiological tasks. These algorithms, called image segmentation algorithms, play a vital role in numerous biomedical-imaging applications, such as the quantification of tissue volumes (1), diagnosis (2), localization of pathology (3), study of anatomical structure (4), treatment planning (5), and computer-integrated surgery (6).

This chapter provides an overview of current methods for computer-assisted or computer-automated segmentation of anatomical medical images. Methods and applications from recent literature are briefly described. A full description of these competing methods is beyond the scope of this chapter, and readers are referred to other references for additional details. We focus instead on providing an introduction to current applications of segmentation in medical imaging and the various issues that must be confronted. Although we refer to only the most commonly used radiological modalities for imaging anatomy, most of the concepts described are applicable to other imaging modalities as well.

BACKGROUND

We first define terminology that is used throughout the review, and we describe important issues in the segmentation of medical images.

Definitions

An image is a collection of measurements in two-dimensional (2-D) or three-dimensional (3-D) space. In medical images, these measurements or 'image intensities' can be radiation absorption in X-ray imaging, acoustic pressure in ultrasound, or radio frequency (RF) signal amplitude in MRI. If a single measurement is made at each location in the image, then the image is called a scalar image. If

more than one measurement is made (e.g. dual-echo MRI), the image is called a vector or multichannel image. Images may be acquired in the continuous domain, such as on X-ray film, or in discrete space as in MRI. In 2-D discrete images, the location of each measurement is called a pixel, and in 3-D images, it is called a voxel. For simplicity, we use "pixel" for both the 2-D and 3-D cases.

Classically, image segmentation is defined as the partitioning of an image into nonoverlapping, constituent regions that are homogeneous with respect to some characteristic such as intensity or texture (7–9). If the domain of the image is given by Ω, then the segmentation problem is to determine the sets $S_k \subset \Omega$, whose union is the entire domain Ω. Thus, the sets that make up a segmentation must satisfy

$$\Omega = \bigcup_{k=1}^{K} S_k \tag{1}$$

where $S_k \cap S_j = \phi$ for $k \neq j$, and each S_k is connected. Ideally, a segmentation method finds those sets that correspond to distinct anatomical structures or regions of interest in the image.

When the constraint that regions be connected is removed, then determining the sets S_k is called pixel classification, and the sets themselves are called classes. Pixel classification, rather than classical segmentation, is often a desirable goal in medical images, particularly when disconnected regions belonging to the same tissue class require identification. Determination of the total number of classes K in pixel classification can be a difficult problem (10). Often, the value of K is assumed to be known based on prior knowledge of the anatomy being considered. For example, in the segmentation of magnetic-resonance (MR) brain images, it is common to assume that the $K = 3$, corresponding to gray-matter, white-matter, and cerebrospinal-fluid tissue classes (11).

Labeling is the process of assigning a meaningful designation to each region or class and can be performed separately from segmentation. It maps the numerical index k of set S_k to an anatomical designation. In medical imaging, the labels are often visually obvious and can be determined on inspection by a physician or technician. Computer-automated labeling is desirable when labels are not obvious and in automated processing systems. A typical situation involving labeling occurs in digital mammography, in which the image is segmented into distinct regions and the regions are subsequently labeled as healthy or tumorous tissue.

Methods that delineate a structure or structures in an image, including both classical segmentation and pixel classification methods, are considered in this review. Although we do not discuss specific labeling methods, we do discuss several techniques that perform both segmentation and labeling simultaneously. Two fields closely related to segmentation that we do not discuss here are feature detection and motion estimation. Feature detection is concerned with determining the presence of some image property, whereas segmentation generally assumes that the property is already present and attempts to precisely localize areas that possess the property. For example, edge detection methods can determine the

location of edges in an image, but, without further processing, these methods do not necessarily extract any region of interest. However, edge detection can be used in conjunction with other methods to form a segmentation algorithm. Motion estimation methods often consist of applying segmentation algorithms to time sequences of images. We consider this application of segmentation to be a separate branch of research and do not include it in this review.

Dimensionality

Dimensionality refers to whether a segmentation method operates in a 2-D image domain or a 3-D image domain. Methods that rely solely on image intensities are independent of the image domain. However, certain methods, such as deformable models, Markov random fields (MRFs), and region growing (described below), incorporate spatial information and may therefore operate differently depending on the dimensionality of the image. Generally, 2-D methods are applied to 2-D images, and 3-D methods are applied to 3-D images. In some cases, however, 2-D methods are applied sequentially to the slices of a 3-D image (12, 13). This may arise because of practical reasons such as ease of implementation, lower computational complexity, and reduced memory requirements. In addition, certain structures are more easily defined along 2-D slices.

A unique situation that occurs in medical-image segmentation is the delineation of regions on a non-Euclidean domain, such as in brain cortex parcellation (14, 15). This is essentially segmentation on a surface of measurements. Because a surface is a 2-D object folded in 3-D space, segmentation on a surface cannot be treated as a standard 2-D or 3-D problem. The modeling of spatial characteristics along a surface is much more difficult than in a standard imaging plane because of the irregular sampling used by mesh representations and because of the need to compute geodesics (16). This is an emerging area of research, and preliminary results have shown great promise particularly for studying brain function and structure.

Soft Segmentation and Partial-Volume Effects

Partial-volume effects are artifacts that occur where multiple tissue types contribute to a single pixel, resulting in a blurring of intensity across boundaries. Figure 1 illustrates how the sampling process can result in partial-volume effects, leading to ambiguities in structural definitions. In Figure 1*b*, it is difficult to precisely determine the boundaries of the two objects. Partial-volume effects are common in medical images, particularly for 3-D CT and MRI data, in which the resolution is not isotropic and, in many cases, is quite poor along one axis of the image. Poor resolution was often ignored in early work involving the segmentation of MR images, but more recently, improved methods to address partial-volume effects, as well as progress toward higher-resolution imaging, have helped to alleviate the situation.

The most common approach to addressing partial-volume effects is to produce segmentations that allow regions or classes to overlap, called soft segmentations.

(*a*) (*b*)

Figure 1 Illustration of partial-volume effect. (*a*) Ideal image. (*b*) Acquired image.

Standard approaches use 'hard segmentations' that enforce a binary decision on whether a pixel is inside or outside the object. Soft segmentations, on the other hand, retain more information from the original image by allowing for uncertainty in the location of object boundaries.

In pixel classification methods, the notion of a soft segmentation stems from the generalization of a set 'characteristic function.' A characteristic function is simply an indicator function denoting whether a pixel is inside or outside its corresponding set. For a location $j \in I$, the characteristic function $\chi_k(j)$ of the set S_k is defined as

$$\chi_k(j) = \begin{cases} 1 & \text{if } j \in S_k \\ 0 & \text{otherwise} \end{cases} \tag{2}$$

Characteristic functions can be generalized to 'membership functions' (17), which need not be binary valued. Membership functions $m_k(j)$ satisfy the following constraints:

$$0 \leq m_k(j) \leq 1, \quad \text{for all } j, k \tag{3}$$

$$\sum_{k=1}^{K} m_k(j) = 1, \quad \text{for all } j \tag{4}$$

The value of a membership function $m_k(j)$ can be interpreted as the contribution of class k to location j. Thus, wherever membership values are greater than zero for two or more classes, those classes are overlapping. Conversely, if the membership function is unity for some value of j and k, then class k is the only contributing class at location j. Membership functions can be derived by using fuzzy clustering and classifier algorithms (18, 19) or statistical algorithms, in which case the membership functions are probability functions (20, 21), or they can be computed as estimates of partial-volume fractions (22). Soft segmentations based on membership functions can be easily converted to hard segmentations by assigning a pixel to its class with the highest membership value.

Intensity Inhomogeneities

A major difficulty that is specific to the segmentation of MR images is the 'intensity inhomogeneity artifact' (23, 24), which causes a shading effect to appear over the image. The artifact can significantly degrade the performance of methods that assume that the intensity value of a tissue class is constant over the image. Although improvements in scanner technology have reduced this artifact somewhat, inhomogeneities remain a problem particularly in images acquired by using surface coils. Figure 2*a* shows an axially acquired MR cardiac image taken from a female subject with a myocardial infarction. Intensity inhomogeneities are noticeable particularly near the breasts. Many approaches have been proposed in the literature for performing tissue classification in the presence of intensity inhomogeneity artifacts. Some methods suggest a prefiltering operation that attempts to remove the inhomogeneity before actual segmentation (cf 25–28). Methods that simultaneously segment the image and estimate the inhomogeneity, however, offer the advantage of being able to use intermediate information gained from the segmentation.

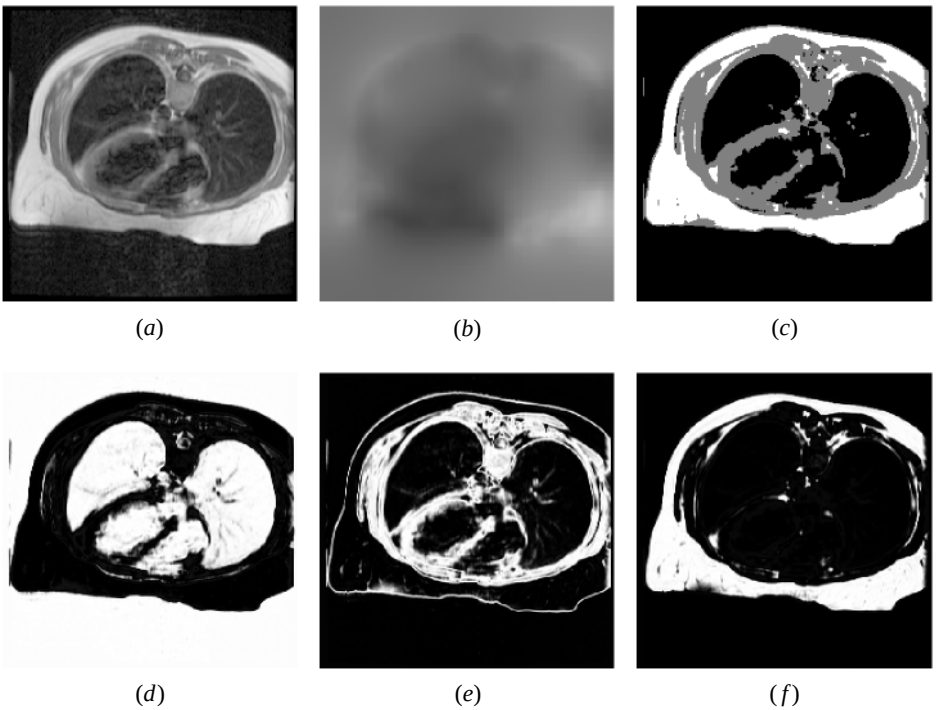

Figure 2 Example of simultaneous inhomogeneity correction and soft segmentation. (*a*) Magnetic resonance heart image acquired with a fast spin echo sequence in a true axial prescription; (*b*) estimated gain field; (*c*) hard segmentation into three classes, (*d–f*) membership functions of the three classes (data provided courtesy of C Constantinides).

There are two prevailing approaches for modeling inhomogeneities in methods that perform simultaneous segmentation. The first approach assumes that the mean intensity for each tissue class is spatially varied and that these mean intensities are independent of one another (11, 29). The second approach models the inhomogeneities as a multiplicative gain field (18) or additive bias field of the image logarithm (21, 30). It is unclear which of these two provides more accurate modeling of inhomogeneity effects, although the second approach has the advantage of being computationally less expensive. The second approach can also be used for removing inhomogeneities by simple multiplication of the acquired image by the reciprocal of the estimated gain field.

Figure 2 shows the results of applying the adaptive fuzzy *c*-means algorithm (18), which performs a soft segmentation while compensating for intensity inhomogeneities. The heart image of Figure 2*a* was segmented into three classes (roughly corresponding to air, to muscle, and to fat and skin, respectively) and Figure 2*d–f* corresponds to the membership functions for those three classes. Figure 2*b* shows the gain field estimated from the original image. The hard segmentation in Figure 2*c* was obtained by using maximum membership classification. Note that the ring artifact present in Figure 2*e* results from partial-volume effects that cause the boundary between fat, skin, and air to have an intensity similar to that of muscle. This effect is common and is a disadvantage of intensity-based pixel classification methods.

Interaction

The tradeoff between manual interaction and performance is an important consideration in any segmentation application. Manual interaction can improve accuracy by incorporating the prior knowledge of an operator. For large-population studies, however, this can be laborious and time-consuming. The type of interaction required by segmentation methods can range from completely manual delineation of an anatomical structure to the selection of a seed point for a region-growing algorithm (see below). The differences in these types of interaction are the amounts of time and effort required, as well as the amounts of training required by operators. Methods that rely on manual interaction can also be vulnerable to reliability issues. However, even automated segmentation methods typically require some interaction for specifying some initial parameters, whose values can significantly affect performance (31).

Validation

To quantify the performance of a segmentation method, validation experiments are necessary. Validation is typically performed with one of two different types of truth models. The most straightforward approach to validation is to compare the automated segmentations with manually obtained segmentations (cf 32). This approach, besides suffering from the drawbacks outlined above, does not guarantee a perfect truth model, because an operator's performance can also be flawed. The

other common approach to validating segmentation methods is through the use of physical phantoms (33) or computational phantoms (34). Physical phantoms provide an accurate depiction of the image acquisition process but typically do not present a realistic representation of anatomy. Computational phantoms can represent anatomy realistically, but usually simulate the image acquisition process by using simplified models.

Once a truth model is available, a figure of merit must be defined for quantifying accuracy or precision (cf 35). The choice of the figure of merit is dependent on the application and can be based on region information, such as the number of pixels misclassified, or boundary information, such as distance to the true boundary. A survey on this topic has been provided (36).

METHODS

Several common approaches have appeared in the recent literature on medical-image segmentation. We define each method, provide an overview of its implementation, and discuss its advantages and disadvantages. Although each technique is described separately, multiple techniques are often used in conjunction for solving different segmentation problems.

We divide segmentation methods into eight categories: (*a*) thresholding approaches, (*b*) region growing approaches, (*c*) classifiers, (*d*) clustering approaches, (*e*) Markov random field (MRF) models, (*f*) artificial neural networks, (*g*) deformable models, and (*h*) atlas-guided approaches. Other notable methods that do not belong to any of these categories are described at the end of this section. Of the methods discussed in this section, thresholding, classifier, clustering, and MRF approaches can be considered pixel classification methods.

Several general surveys on image segmentation exist in the literature (7, 9). Several surveys have targeted segmentation of MR images in particular (3, 37, 38). Direct comparisons of different methods for segmenting MR images are also available (39, 40).

Thresholding

Thresholding approaches segment scalar images by creating a binary partitioning of the image intensities. Figure 3*a* shows the histogram of a scalar image that possesses three apparent classes, corresponding to the three modes. A thresholding procedure attempts to determine an intensity value, called the threshold, which separates the desired classes. The segmentation is then achieved by grouping all pixels with intensities greater than the threshold into one class and all other pixels into another class. Two potential thresholds are shown in Figure 3*a* at the valleys of the histogram. Determination of more than one threshold value is a process called multithresholding (41).

Thresholding is a simple yet often effective means for obtaining a segmentation of images in which different structures have contrasting intensities or other

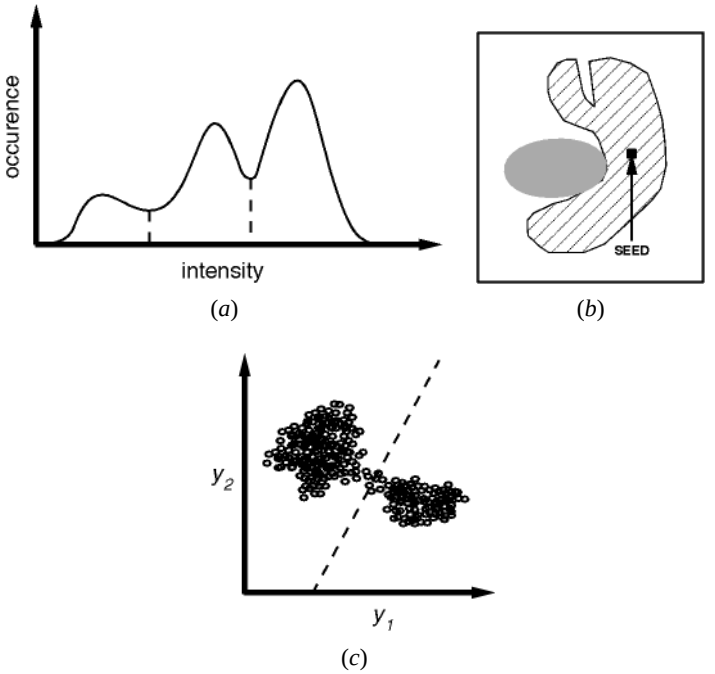

Figure 3 Feature space methods and region growing. (*a*) Histogram showing three apparent classes. (*b*) 2-D feature space. (*c*) Example of region growing.

quantifiable features. The partition is usually generated interactively, although automated methods do exist (41). Thresholding is often performed interactively, based on the operator's visual assessment of the resulting segmentation.

Thresholding is often used as an initial step in a sequence of image-processing operations (cf 42, 43). It has been applied in digital mammography, in which two classes of tissue are typically present—healthy and tumorous (44, 45). Its main limitations are that, in its simplest form, only two classes are generated, and it cannot be applied to multichannel images. In addition, thresholding typically does not take into account the spatial characteristics of an image. This causes it to be sensitive to noise and intensity inhomogeneities, which can occur in MR images. Both of these artifacts essentially corrupt the histogram of the image, making separation more difficult. For these reasons, variations on classical thresholding have been proposed for medical-image segmentation that incorporate information based on local intensities (46) and connectivity (47). A survey on thresholding techniques is provided elsewhere (41).

Region Growing

Region growing is a technique for extracting an image region that is connected based on some predefined criteria. These criteria can be based on intensity

information and/or edges in the image (7). In its simplest form, region growing requires a seed point that is manually selected by an operator and extracts all pixels connected to the initial seed based on some predefined criteria. For example, one possible criterion might be to grow the region until an edge in the image is met. This is depicted in Figure 3*b*, in which region growing has been used to isolate one of the structures from Figure 1*a*.

Like thresholding, region growing is seldom used alone but usually within a set of image-processing operations, particularly for the delineation of small, simple structures such as tumors and lesions (48, 49). The primary disadvantage of region growing is that it requires manual interaction to obtain the seed point. Thus, for each region that needs to be extracted, a seed must be planted. Split-and-merge is an algorithm related to region growing, but it does not require a seed point (50). Region growing can also be sensitive to noise, causing extracted regions to have holes or even become disconnected. Conversely, partial-volume effects can cause separate regions to become connected. To help alleviate these problems, a homotopic region-growing algorithm has been proposed that preserves the topology between an initial region and an extracted region (51). Fuzzy analogies to region growing have also been developed (52).

Classifiers

Classifier methods are pattern recognition techniques that seek to partition a feature space derived from the image by using data with known labels (37, 53). A feature space is the range space of any function of the image, with the most common feature space being the image intensities themselves. A histogram, as shown in Figure 3*a*, is an example of a one-dimensional feature space. Figure 3*c* shows an example of a partitioned 2-D feature space with two apparent classes. Such a feature space might have been generated from a dual-echo MR image, in which one axis represents the intensities of the proton density-weighted image and the other axis represents the intensities of the T_2-weighted image. All pixels with their associated features on the left side of the partition would be grouped into one class.

Classifiers are known as supervised methods because they require training data that are manually segmented and then used as references for automatically segmenting new data. There are a number of ways in which training data can be applied in classifier methods. A simple classifier is the nearest-neighbor classifier, in which each pixel is classified in the same class as the training datum with the closest intensity. The *k*-nearest-neighbor classifier is a generalization of this approach, in which the pixel is classified into the same class as the majority of the *k*-closest training data. The *k*-nearest-neighbor classifier is considered a nonparametric classifier because it makes no underlying assumption about the statistical structure of the data. Another nonparametric classifier is the Parzen window, in which the classification is made by a weighted decision process within a predefined window of the feature space, centered at the unlabeled pixel intensity.

A commonly used parametric classifier is the maximum-likelihood or Bayes classifier. It assumes that the pixel intensities are independent samples from a mixture of probability distributions, usually Gaussian. This mixture, called a finite-mixture model, is given by the probability density function

$$f(y_j; \theta, \pi) = \sum_{k=1}^{K} \pi_k f_k(y_j; \theta_k) \quad (5)$$

where y_j is the intensity of pixel j, f_k is a component probability density function parameterized by θ_k, and $\theta = [\theta_1, \ldots, \theta_K]$. The variables π_k are mixing coefficients that weight the contribution of each density function and $\pi = [\pi_1, \ldots, \pi_K]$. Training data are collected by obtaining representative samples from each component of the mixture model and then estimating each θ_k accordingly. For Gaussian mixtures, this means estimating K-means, covariances, and mixing coefficients. Classification of new data is obtained by assigning each pixel to the class with the highest posterior probability. When the data truly follow a finite Gaussian mixture distribution, the maximum-likelihood classifier can perform well and is capable of providing a soft segmentation composed of the posterior probabilities. Additional parametric and nonparametric classifiers are described in Reference 3.

Standard classifiers require that the structures to be segmented possess distinct quantifiable features. Because training data can be labeled, classifiers can transfer these labels to new data as long as the feature space sufficiently distinguishes each label as well. Being noniterative, classifiers are relatively computationally efficient, and, unlike thresholding methods, they can be applied to multichannel images (54). A disadvantage of classifiers is that they generally do not perform any spatial modeling. This weakness has been addressed in recent work extending classifier methods to segmenting images that are corrupted by intensity inhomogeneities (21). Neighborhood and geometric information was also incorporated into a classifier approach in Reference 55. Another disadvantage is the requirement of manual interaction to obtain training data. Training sets can be acquired for each image that requires segmenting, but this can be time consuming and laborious. On the other hand, use of the same training set for a large number of scans can lead to biased results that do not take into account anatomical and physiological variability between different subjects.

Clustering

Clustering algorithms essentially perform the same function as classifier methods without the use of training data. Thus, they are termed unsupervised methods. To compensate for the lack of training data, clustering methods iteratatively alternate between segmenting the image and characterizing the properties of each class. In a sense, clustering methods train themselves, using the available data.

Three commonly used clustering algorithms are the K-means or ISODATA algorithm (56), the fuzzy c-means algorithm (37), and the expectation-maximization

(EM) algorithm (33, 57). The K-means clustering algorithm clusters data by iteratively computing a mean intensity for each class and segmenting the image by classifying each pixel in the class with the closest mean (58). Figure 4*b* shows the result of applying the K-means algorithm to a slice of an MR brain image in Figure 4*a*. The number of classes was assumed to be three, representing (from dark gray to white in Figure 4) cerebrospinal fluid, gray matter, and white matter. The fuzzy c-means algorithm generalizes the K-means algorithm, allowing for soft segmentations based on fuzzy set theory (17). The EM algorithm applies the same clustering principles with the underlying assumption that the data follow a Gaussian mixture model (see Equation 5). It iterates between computing

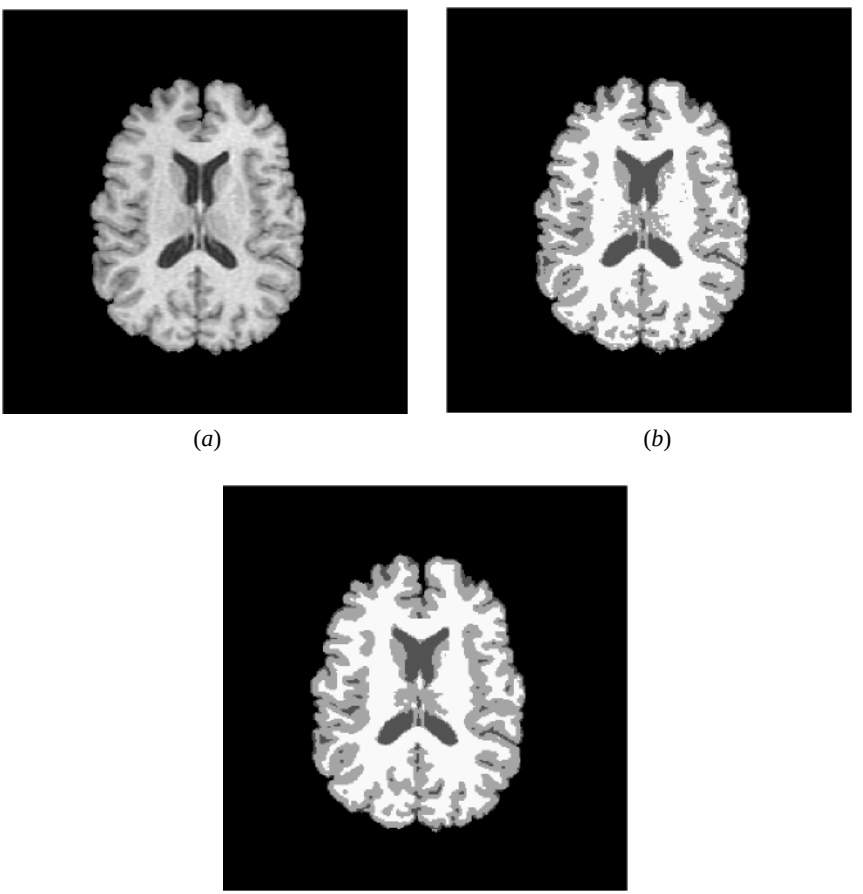

(*a*) (*b*)

(*c*)

Figure 4 Segmentation of a magnetic resonance brain image. (*a*) Original image. (*b*) Segmentation using the K-means algorithm. (*c*) Segmentation using the K-means algorithm with a Markov random field prior.

the posterior probabilities and computing maximum likelihood estimates of the means, covariances, and mixing coefficients of the mixture model.

Although clustering algorithms do not require training data, they do require an initial segmentation (or, equivalently, initial parameters). The EM algorithm has demonstrated greater sensitivity to initialization than the K-means or fuzzy c-means algorithm (31). Like classifier methods, clustering algorithms do not directly incorporate spatial modeling and can therefore be sensitive to noise and intensity inhomogeneities. This lack of spatial modeling, however, can provide significant advantages for fast computation (59). Work on improving the robustness of clustering algorithms to intensity inhomogeneities in MR images has demonstrated excellent success (11, 18). Robustness to noise can be incorporated by MRF modeling as described in the next section.

Markov Random Field Models

MRF modeling itself is not a segmentation method but a statistical model that can be used within segmentation methods. MRFs model spatial interactions between neighboring or nearby pixels. These local correlations provide a mechanism for modeling a variety of image properties (60). In medical imaging, they are typically used because most pixels belong to the same class as their neighboring pixels. In physical terms, this implies that any anatomical structure that consists of only one pixel has a very low probability of occurring under an MRF assumption.

MRFs are often incorporated into clustering segmentation algorithms such as the K-means algorithm under a Bayesian prior model (11, 29, 30). The segmentation is then obtained by maximizing the a posteriori probability of the segmentation, given the image data. This maximization can be achieved by iterative methods such as iterated conditional modes (61) or simulated annealing (62). Figure 4*c* shows the robustness to noise in a segmentation resulting from an MRF prior. The segmentation does not exhibit as many small, disconnected regions as the non-MRF result of Figure 4*b*.

A difficulty associated with MRF models is proper selection of the parameters controlling the strength of spatial interactions (60). A setting that is too high can result in an excessively smooth segmentation and a loss of important structural details. In addition, MRF methods usually require computationally intensive algorithms. Despite these disadvantages, MRFs are widely used not only to model segmentation classes, but also to model intensity inhomogeneities that can occur in MR images (30) and textural properties, which is useful in the segmentation of digital mammograms (63).

Artificial Neural Networks

Artificial neural networks (ANNs) are parallel networks of processing elements or nodes that simulate biological learning. Each node in an ANN is capable of performing elementary computations. Learning is achieved through the adaptation

of weights assigned to the connections between nodes. A thorough treatment on neural networks can be found in References 64 and 65.

ANNs represent a paradigm for machine learning and can be used in a variety of ways for image segmentation. The most widely applied use in medical imaging is as a classifier (40, 66), in which the weights are determined by using training data and the ANN is then used to segment new data. ANNs can also be used in an unsupervised fashion as a clustering method (37, 67), as well as for deformable models (68). Because of the many interconnections used in a neural network, spatial information can be easily incorporated into its classification procedures. Although ANNs are inherently parallel, their processing is usually simulated on a standard serial computer, thus reducing this potential computational advantage.

Deformable Models

Deformable models are physically motivated, model-based techniques for delineating region boundaries by using closed parametric curves or surfaces that deform under the influence of internal and external forces. To delineate an object boundary in an image, a closed curve or surface must first be placed near the desired boundary and then allowed to undergo an iterative relaxation process. Internal forces are computed from within the curve or surface to keep it smooth throughout the deformation. External forces are usually derived from the image to drive the curve or surface toward the desired feature of interest. Figure 5 shows an example of applying a 2-D deformable model or 'active contour' to an MR heart image. In Figure 5*b*, the active contour was initialized as a circle and then allowed to deform to the inner boundary of the left ventricle.

Deformable models have been widely applied in the segmentation of medical images. One area in which they are used often is the reconstruction of the cerebral

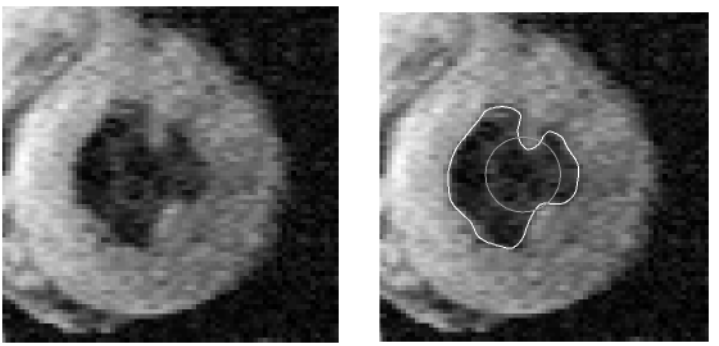

(*a*) (*b*)

Figure 5 Extraction of the inner wall of the left ventricle from a magnetic resonance image using active contours. (*a*) Original image. (*b*) Initial active contour and the final converged result.

cortex from MR images (69–71). An example of using a deformable surface model for this application is shown in Figure 6 (see color insert). A view of the intersection between this surface and orthogonal slices of the MR image volume is given in Figure 7 (see color insert). Deformable models have also been used in the segmentation of cardiac images (72), bone in CT images (73), and ultrasound (74). The dynamic nature of deformable models make tham especially well suited to motion-tracking tasks, which are common in ultrasound imaging.

The main advantages of deformable models are their ability to directly generate closed parametric curves or surfaces from images and their incorporation of a smoothness constraint that provides robustness to noise and spurious edges. A disadvantage is that they require manual interaction to place an initial model and choose appropriate parameters. Reducing sensitivity to initialization has been a topic of research that has demonstrated excellent success (75–78). Standard deformable models can also exhibit poor convergence to concave boundaries. This difficulty can be alleviated somewhat through the use of pressure forces (75) and other modified external-force models (78). Another important extension of deformable models is the adaptivity of model topology by using an implicit representation rather than an explicit parameterization (76, 77, 79). A general review on deformable models in medical image analysis can be found in reference 80.

Atlas-Guided Approaches

Atlas-guided approaches are a powerful tool for medical-image segmentation when a standard atlas or template is available. The atlas is generated by compiling information on the anatomy that requires segmenting. This atlas is then used as a reference frame for segmenting new images. Conceptually, atlas-guided approaches are similar to classifiers except that they are implemented in the spatial domain of the image rather than in a feature space.

The standard atlas-guided approach treats segmentation as a registration problem (see 81 for a detailed survey on registration techniques). It first finds a one-to-one transformation that maps a presegmented atlas image to the target image that requires segmenting. This process is often referred to as ‘atlas warping.’ The warping can be performed with linear (82–84) transformations, but, because of anatomical variability, a sequential application of linear and nonlinear (15, 85–87) transformations is often used. An example of atlas warping for an MR head scan is shown in Figure 8 (87). Because the atlas is already segmented, all structural information is transferred to the target image. This is shown in Figure 9, in which the Talairach brain atlas (82) has been mapped to an MR image (86).

Atlas-guided approaches have been applied mainly in MR brain imaging for segmentation of various structures (85), as well as for extracting the brain volume from head scans (88). An advantage of atlas-guided approaches is that labels are transferred as well as the segmentation. They also provide a standard system for studying morphometric properties (89, 90). Even with nonlinear registration methods, however, finding accurate segmentations of complex structures is difficult

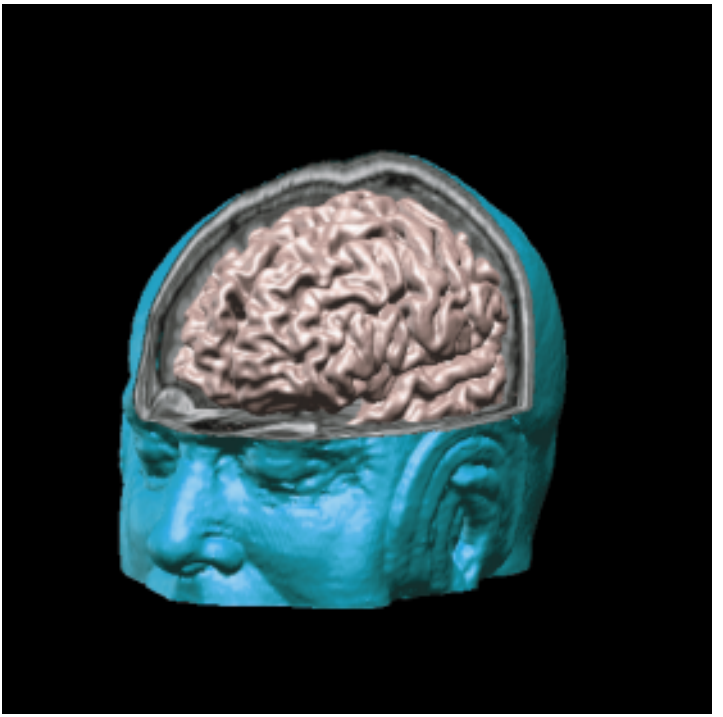

Figure 6 An example of using a deformable surface in the reconstruction of the cerebral cortex.

Figure 7 A view of the intersection between the deformable surface and orthogonal slices of the MR image.

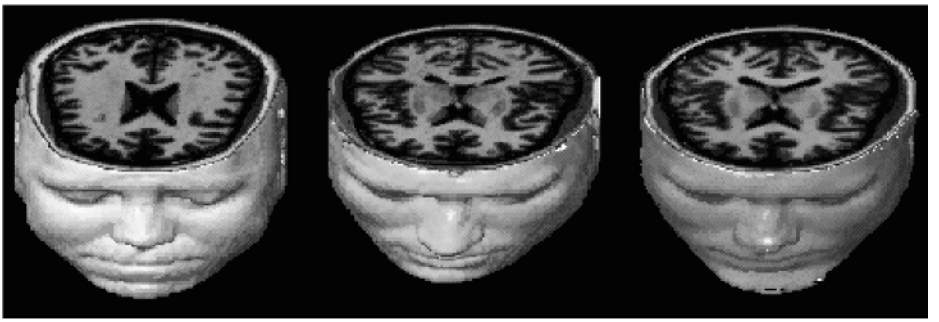

Figure 8 Demonstration of atlas warping. (*a*) Template image; (*b*) target image; (*c*) warped template. (Images provided courtesy of GE Christensen and MI Miller.)

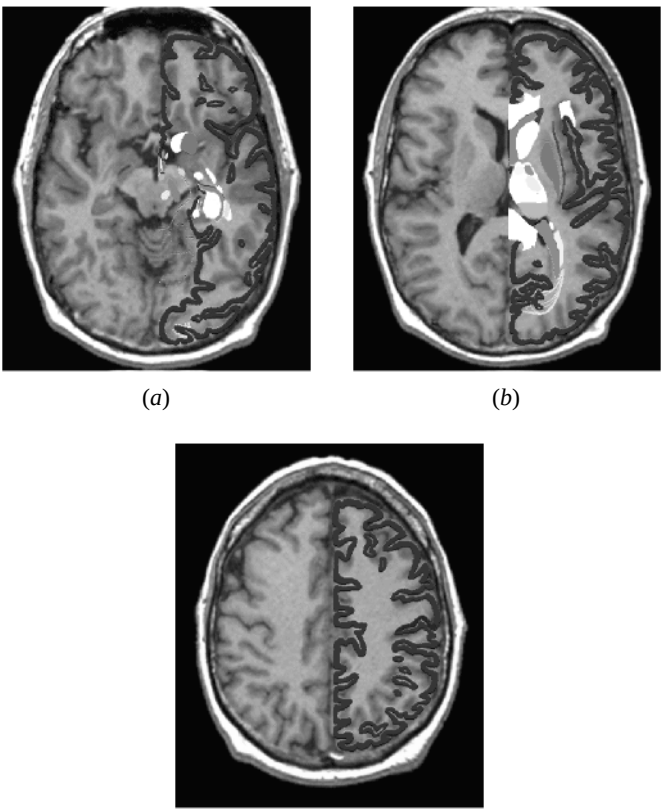

Figure 9 Three slices from a magnetic resonance brain volume overlaid with a warped atlas. (Images provided courtesy of CA Davatzikos.)

owing to anatomical variability. This is shown in Figure 9, in which the cerebral cortex is not segmented as accurately as shown in Figure 4. Thus, atlas-guided approaches are generally better suited for segmentation of structures that are stable over the population of study. One method that helps model anatomical variability is the use of probabilistic atlases (89), but these require additional time and interaction to accumulate data. Another method is the use of manually selected landmarks to constrain transformation (86).

Other Approaches

Model-fitting is a segmentation method that typically fits a simple geometric shape such as an ellipse or parabola to the locations of extracted image features in an image (91). This technique is specialized to the structure being segmented but is easily implemented and can provide good results when the model is appropriate. A more general approach is to fit spline curves or surfaces (92) to the features. The main difficulty with model-fitting is that image features must first be extracted before the fitting can take place.

The watershed algorithm uses concepts from edge detection and mathematical morphology (8) to partition images into homogeneous regions (93). The method can suffer from oversegmentation, which occurs when the image is segmented into an unnecessarily large number of regions. Thus, watershed algorithms in medical imaging are usually followed by a post-processing step to merge separate regions that belong to the same structure (94).

Figure 10 shows an example in which a mammogram is initially oversegmented by using a watershed algorithm. A statistical classifier (95) is then used to determine which regions contain microcalcifications. This classification step is typically performed based on textural properties. Note that a perfect delineation of microcalcifications and masses in mammograms is difficult but not often necessary because detection is the primary goal.

CONCLUSION

Future research in the segmentation of medical images will strive toward improving the accuracy, precision, and computational speed of segmentation methods, as well as reducing the amount of manual interaction. Accuracy and precision can be improved by incorporating prior information from atlases and by combining discrete and continuous spatial-domain segmentation methods. For increasing computational efficiency, multiscale processing (cf 96) and parallelizable methods such as neural networks are promising approaches. Computational efficiency will be particularly important in real-time processing applications.

Possibly the most important question surrounding the use of image segmentation is its application in clinical settings. Computerized segmentation methods

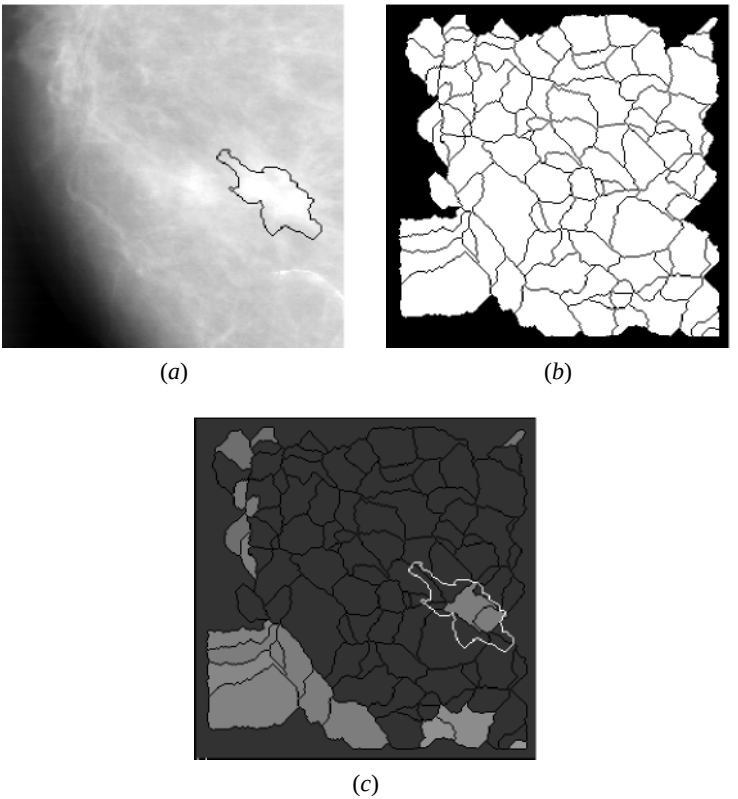

Figure 10 Segmentation in digital mammography. (*a*) Digitized mammogram and radiologist's boundary for biopsy-proven malignant tumor. (*b*) Result of watershed algorithm. (*c*) Suspicious regions determined by automated method. (Images provided courtesy of CE Priebe.)

have already demonstrated their utility in research applications and are now garnering increased use for computer-aided diagnosis and radiotherapy planning. For segmentation methods to gain acceptance in routine clinical applications, extensive validation is required on the particular methods in question. Furthermore, one must be able to demonstrate some significant performance advantage (e.g. more accurate diagnosis or earlier detection of pathology) over traditional methods to warrant the training and equipment costs associated with using computerized methods. It is unlikely that automated segmentation methods will ever replace physicians, but they will likely become crucial elements of medical-image analysis. Segmentation methods will be particularly valuable in areas such as image-guided surgery, in which visualization of the anatomy is a critical component.

LITERATURE CITED

1. Larie SM, Abukmeil SS. 1998. Brain abnormality in schizophrenia: a systematic and quantitative review of volumetric magnetic resonance imaging studies. *J. Psychol.* 172:110–20
2. Taylor P. 1995. Invited review: computer aids for decision-making in diagnostic radiology—a literature review. *Br. J. Radiol.* 68:945–57
3. Zijdenbos AP, Dawant BM. 1994. Brain segmentation and white matter lesion detection in MR images. *Crit. Rev. Biomed. Eng.* 22:401–65
4. Worth AJ, Makris N, Caviness VS, Kennedy DN. 1997. Neuroanatomical segmentation in MRI: technological objectives. *Int. J. Pattern Recognit. Artif. Intell.* 11:1161–87
5. Khoo VS, Dearnaley DP, Finnigan DJ, Padhani A, Tanner SF, Leach MO. 1997. Magnetic resonance imaging (MRI): considerations and applications in radiotherapy treatment planning. *Radiother. Oncol.* 42:1–15
6. Grimson WEL, Ettinger GJ, Kapur T, Leventon ME, Wells WM, et al. 1997. Utilizing segmented MRI data in image-guided surgery. *Int. J. Pattern Recognit. Artif. Intell.* 11:1367–97
7. Haralick RM, Shapiro LG. 1985. Image segmentation techniques. *Comput. Vis. Graph. Image Proc.* 29:100–32
8. Gonzalez RC, Woods RE. 1992. *Digital Image Processing.* Reading, MA: Addison-Wesley. 716 pp.
9. Pal NR, Pal SK. 1993. A review on image segmentation techniques. *Pattern Recognit.* 26:1277–94
10. Langan DA, Modestino JW, Zhang J. 1998. Cluster validation for unsupervised stochastic model-based image segmentation. *IEEE Trans. Image Process.* 7:180–95
11. Rajapakse JC, Giedd JN, Rapoport JL. 1997. Statistical approach to segmentation of single-channel cerebral MR images. *IEEE Trans. Med. Imaging* 16:176–86
12. Pham DL, Prince JL, Dagher AP, Xu C. 1997. An automated technique for statistical characterization of brain tissues in magnetic resonance imaging. *Int. J. Pattern Recognit. Artif. Intell.* 11(8):1189–211
13. Ge Y, Fitzpatrick JM, Dawant BM, Bao J, Kessler RM, Margolin R. 1996. Accurate localization of cortical convolutions in MR brain images. *IEEE Trans. Med. Imaging* 15:418–28
14. Rademacher J, Galaburda AM, Kennedy DN, Filipek PA, Caviness VS. 1992. Human cerebral cortex: localization, parcellation and morphometry with magnetic resonance imaging. *J. Cogn. Neurosci.* 4:352–74
15. Sandor S, Leahy R. 1997. Surface-based labeling of cortical anatomy using a deformable atlas. *IEEE Trans. Med. Imaging* 16:41–54
16. Khaneja N, Miller MI, Grenander U. 1998. Dynamic programming generation of curves on brain surfaces. *IEEE Trans. Pattern Anal. Mach. Intell.* 20:1260–65
17. Zadeh LA. 1965. Fuzzy sets. *Inf. Control* 8:338–53
18. Pham DL, Prince JL. 1999. An adaptive fuzzy c-means algorithm for image segmentation in the presence of intensity inhomogeneities. *Pattern Recognit. Lett.* 20:57–68
19. Herndon RC, Lancaster JL, Toga AW, Fox PT. 1996. Quantification of white matter and gray matter volumes from T1 parametric images using fuzzy classifiers. *J. Magn. Reson. Imaging* 6:425–35
20. Liang Z. 1993. Tissue classification and segmentation of MR images. *IEEE Eng. Med. Biol.* 12:81–85

21. Wells WM, Grimson WEL, Kikins R, Jolesz FA. 1996. Adaptive segmentation of MRI data. *IEEE Trans. Med. Imaging* 15:429–42
22. Choi HS, Hanynor DR, Kim Y. 1991. Partial volume tissue classification of multichannel magnetic resonance images—a mixel model. *IEEE Trans. Med. Imaging* 10:395–407
23. Simmons A, Tofts PS, Barker GJ, Arridge SR. 1994. Sources of intensity nonuniformity in spin echo images at 1.5T. *Magn. Reson. Med.* 32:121–28
24. Sled JG, Pike GB. 1998. Standing-wave and RF penetration artifacts caused by elliptic geometry: an electrodynamic analysis of MRI. *IEEE Trans. Med. Imaging* 17:653–62
25. Dawant BM, Zijidenbos AP, Margolin RA. 1993. Correction of intensity variations in MR images for computer-aided tissue classification. *IEEE Trans. Med. Imaging* 12:770–81
26. Meyer CR, Peyton HB, Pipe J. 1995. Retrospective correction of intensity inhomogeneities in MRI. *IEEE Trans. Med. Imaging* 14:36–41
27. Brinkmann BH, Manduca A, Robb RA. 1998. Optimized homomorphic unsharp masking for MR grayscale inhomogeneity correction. *IEEE Trans. Med. Imaging* 17:161–71
28. Sled JG, Zijdenbos AP, Evans AC. 1998. A nonparametric method for automatic correction of intensity nonuniformity in MRI data. *IEEE Trans. Med. Imaging* 17:87–97
29. Pappas TN. 1992. An adaptive clustering algorithm for image segmentation. *IEEE Trans. Signal Process.* 40:901–14
30. Held K, Kops ER, Krause BJ, Wells WM, Kikinis R, et al. 1997. Markov random field segmentation of brain MR images. *IEEE Trans. Med. Imaging* 16(6):878–86
31. Davenport JW, Bezdek JC, Hathaway RJ. 1988. Parameter estimation for finite mixture distributions. *Comput. Math. Appl.* 15:810–28
32. Wust P, Gellermann J, Beier J, Wegner S, Tilly W, et al. 1998. Evaluation of segmentation algorithms for generation of patient models in radiofrequency hyperthermia. *Phys. Med. Biol.* 43:3295–307
33. Lei T, Sewchand W. 1992. Statistical approach to X-ray CT imaging and its applications in image analysis. II. A new stochastic model-based image segmentation technique for X-ray CT image. *IEEE Trans. Med. Imaging* 11(1):62–69
34. Collins DL, Zijdenbos AP, Kollokian V, Sled JG, Kabani NJ, et al. 1998. Design and construction of a realistic digital brain phantom. *IEEE Trans. Med. Imaging* 17:463–68
35. Chalana V, Kim Y. 1997. A methodology for evaluation of boundary detection algorithms on medical images. *IEEE Trans. Med. Imaging* 16:642–52
36. Zhang YJ. 1996. A survey of evaluation methods for image segmentation. *Pattern Recognit. Lett.* 29:1335–46
37. Bezdek JC, Hall LO, Clarke LP. 1993. Review of MR image segmentation techniques using pattern recognition. *Med. Phys.* 20:1033–48
38. Clarke LP, Velthuizen RP, Camacho MA, Heine JJ, Vaidyanathan M, et al. 1995. MRI segmentation: methods and applications. *Magn. Reson. Imaging* 13:343–68
39. Vaidyanathan M, Clarke LP, Velthuizen RP, Phuphanich S, Bensaid AM, et al. 1995. Comparison of supervised MRI segmentation methods for tumor volume determination during therapy. *Magn. Reson. Imaging* 13:719–28
40. Hall LO, Bensaid AM, Clarke LP, Velthuizen RP, Silbiger MS, Bezdek JC. 1992. A comparison of neural network and fuzzy clustering techniques in segmenting magnetic resonance images of the brain. *IEEE Trans. Neural Netw.* 3:672–82
41. Sahoo PK, Soltani S, Wong AKC. 1988. A survey of thresholding techniques. *Comput. Vis. Graph. Image Proc.* 41:233–60
42. Singleton HR, Pohost GM. 1997. Auto-

matic cardiac MR image segmentation using edge detection by tissue classification in pixel neighborhoods. *Magn. Reson. Med.* 37:418–24

43. Gordon CL, Webber CE, Adachi JD, Christoforou N. 1996. In vivo assessment of trabecular bone structure at the distal radius from high-resolution computed tomography images. *Phys. Med. Biol.* 41: 495–508
44. Polakowski WE, Cournoyer DA, Rogers SK, DeSimio MP, Ruck DW, et al. 1997. Computer-aided breast cancer detection and diagnosis of masses using difference of Gaussians and derivative-based feature saliency. *IEEE Trans. Med. Imaging* 16:811–19
45. Cheng H, Lui YM, Freimanis RI. 1998. A novel approach to microcalcification detection using fuzzy logic technique. *IEEE Trans. Med. Imaging* 17:442–50
46. Li HD, Kallergi M, Clarke LP, Jain VK, Clark RA. 1995. Markov random field for tumor detection in digital mammography. *IEEE Trans. Med. Imaging* 14:565–76
47. Lee C, Hun S, Ketter TA, Unser M. 1998. Unsupervised connectivity-based thresholding segmentation of midsaggital brain MR images. *Comput. Biol. Med.* 28:309–38
48. Gibbs P, Buckley DL, Blackband SJ, Horsman A. 1996. Tumour volume detection from MR images by morphological segmentation. *Phys. Med. Biol.* 41:2437–46
49. Pohlman S, Powell KA, Obuchowski NA, Chilcote WA, Broniatowski SG. 1996. Quantitative classification of breast tumors in digitized mammograms. *Med. Phys.* 23:1337–45
50. Manousakas IN, Undrill PE, Cameron GG, Redpath TW. 1998. Split-and-merge segmentation of magnetic resonance medical images: performance evaluation and extension to three dimensions. *Comput. Biomed. Res.* 31:393–412
51. Mangin JF, Frouin V, Bloch I, Regis J, Krahe J, Lopez. 1995. From 3D magnetic resonance images to structural representations of the cortex topography using topology preserving deformations. *J. Math. Imaging Vis.* 5:297–318
52. Udupa JK, Samarasekera S. 1996. Fuzzy connectedness and object definition: theory, algorithms and applications in image segmentation. *Graph. Models Image Process.* 58(3):246–61
53. Schalkoff RJ. 1992. *Pattern Recognition: Statistical, Structural and Neural Approaches*. New York: Wiley & Sons. 364 pp.
54. Vannier MW, Butterfield RL, Jordan D, Murphy WA, Levitt RG, Gado M. 1985. Multispectral analysis of magnetic resonance images. *Radiology* 154:221–24
55. Kapur T, Grimson WEL, Kikinis R, Wells WM. 1998. Enhanced spatial priors for segmentation of magnetic resonance imagery In *Proc. Int. Conf. Med. Image Comput. Comp. Assist. Interv., 1st, Cambridge, MA*, pp. 457–68. Berlin: Springer-Verlag
56. Coleman GB, Andrews HC. 1979. Image segmentation by clustering. *Proc. IEEE* 5:773–85
57. Liang Z, MacFall JR, Harrington DP. 1994. Parameter estimation and tissue segmentation from multispectral MR images. *IEEE Trans. Med. Imaging* 13:441–49
58. Jain AK, Dubes RC. 1988. *Algorithms for Clustering Data*. Englewood Cliffs, NJ: Prentice Hall. 696 pp.
59. Hebert TJ. 1997. Fast iterative segmentation of high resolution medical images. *IEEE Trans. Nucl. Sci.* 44:1363–67
60. Li SZ. 1995. *Markov Random Field Modeling in Computer Vision.* Berlin/New York: Springer-Verlag. 264 pp.
61. Besag J. 1986. On the statistical analysis of dirty pictures. *CVGIP: Image Underst.* 57:359–72
62. Geman S, Geman D. 1984. Stochastic relaxation, Gibbs distributions, and the Bayesian restoration of images. *IEEE Trans. Pattern Anal. Mach. Intell.* 6:721–41

63. Chen CH, Lee GG. 1997. On digital mammogram segmentation and microcalcification detection using multiresolution wavelet analysis. *Graph. Models Image Process.* 59:349–64
64. Clark JW. 1991. Neural network modelling. *Phys. Med. Biol.* 36:1259–317
65. Haykin S. 1994. *Neural Networks: A Comprehensive Foundation*. New York: Macmillan. 696 pp.
66. Gelenbe E, Feng Y, Krishnan KRR. 1996. Neural network methods for volumetric magnetic resonance imaging of the human brain. *Proc. IEEE* 84:1488–96
67. Reddick WE, Glass JO, Cook EN, Elkin TD, Deaton RJ. 1997. Automated segmentation and classification of multispectral magnetic resonance images of brain using artificial neural networks. *IEEE Trans. Med. Imaging* 16:911–18
68. Vilarino DL, Brea VM, Cabello D, Pardo JM. 1998. Discrete-time CNN for image segmentation by active contours. *Pattern Recognit. Lett.* 19:721–34
69. Davatzikos C, Bryan RN. 1996. Using a deformable surface model to obtain a shape representation of the cortex. *IEEE Trans. Med. Imaging* 15:785–95
70. McInerney T, Terzopoulos D. 1997. Medical image segmentation using topologically adaptable surfaces. *Lect. Notes Comput. Sci.* 1205:23–32
71. Xu C, Pham DL, Prince JL, Etemad ME, Yu D. 1998. Reconstruction of the central layer of the human cerebral cortex from MR images. In *Proc. Int. Conf. Med. Image Comput. Comp. Assist. Interv., 1st, Cambridge, MA*, pp. 482–88
72. Bardinet E, Cohen LD, Ayache N. 1998. A parametric deformable model to fit unstructured 3D data. *Comput. Vis. Image Underst.* 71:39–54
73. Neumann A, Lorenz C. 1998. Statistical shape model based segmentation of medical images. *Comput. Med. Image Graph.* 22:133–43
74. Mikic I, Krucinski S, Thomas JD. 1998. Segmentation and tracking in echocardiographic sequences: active contours guided by optical flow estimates. *IEEE Trans. Med. Imaging* 17:274–84
75. Cohen LD. 1991. On active contour models and balloons. *CVGIP: Image Underst.* 53:211–18
76. Caselles V, Catte F, Coll T, Dibos F. 1993. A geometric model for active contours. *Numer. Math.* 66:1–31
77. Malladi R, Sethian JA, Vemuri BC. 1995. Shape modeling with front propagation: a level set approach. *IEEE Trans. Pattern Anal. Mach. Intell.* 17:158–75
78. Xu C, Prince JL. 1998. Snakes, shapes, and gradient vector flow. *IEEE Trans. Image Process.* 7:359–69
79. McInerney T, Terzopoulos D. 1995. Topologically adaptable snakes. In *Proc. Int. Conf. Comput. Vis. 5th, Cambridge, MA*, pp. 840–45. Los Alamitos, CA: IEEE Comput. Soc.
80. McInerney T, Terzopoulos D. 1996. Deformable models in medical image analysis: a survey. *Med. Image Anal.* 1:91–108
81. Maintz JBA, Viergever MA. 1998. A survey of medical image registration. *Med. Image Anal.* 2:1–36
82. Talairach J, Tournoux P. 1988. *Co-Planar Stereotaxic Atlas of the Human Brain. 3-Dimensional Proportional System: An Approach to Cerebral Imaging*. Stuttgart, Ger. Thieme. 122 pp.
83. Lancaster JL, Rainey LH, Summerlin JL, Freitas CS, Fox PT, et al. 1997. Automated labeling of the human brain: a preliminary report on the development and evaluation of a forward-transform method. *Hum. Brain Mapp.* 5:238–42
84. Rajarethinam NC, Andreasen R, Cizadlo T, Arndt S, Swayze VW, et al. 1996. Automatic atlas-based volume estimation of human brain regions from MR images. *J. Comput. Assist. Tomogr.* 20:98–106
85. Collins DL, Holmes CJ, Peters TM, Evans AC. 1995. Automatic 3-D model-based

neuroanatomical segmentation. *Hum. Brain Mapp.* 3:190–208
86. Davatzikos C. 1996. Spatial normalization of 3D images using deformable models. *J. Comput. Assist. Tomogr.* 20:656–65
87. Christensen GE, Joshi SC, Miller MI. 1997. Volumetric transformation of brain anatomy. *IEEE Trans. Med. Imag.* 16:864–77
88. Aboutanos GB, Dawant BM. 1997. Automatic brain segmentation and validation: image-based versus atlas-based deformable models. In *SPIE Proc. Med. Imag*. 3034:299–310
89. Thompson P, Toga AW. 1997. Detection, visualization and animation of abnormal anatomic structure with a probabilistic brain atlas based on random vector field transformations. *Med. Image Anal.* 1:271–94
90. Joshi SC, Miller MI, Grenander U. 1997. On the geometry and shape of brain submanifolds. *Int. J. Pattern Recognit. Artif. Intell.* 11:1317–43
91. Pathak SD, Grimm PD, Chalana V, Kim Y. 1998. Pubic arch detection in transrectal ultrasound guided prostate cancer therapy. *IEEE Trans. Med. Imaging* 17:762–71
92. Bae KT, Giger ML, Chen C, Kahn CE. 1993. Automatic segmentation of liver structure in CT images. *Med. Phys.* 20:71–78
93. Vincent L, Soille P. 1991. Watersheds in digital spaces: an efficient algorithm based on immersion simulation. *IEEE Trans. Pattern Anal. Mach. Intell.* 13:583–98
94. Sijbers J, Scheunders P, Verhoye M, Van Der Linden A, Van Dyck D, et al. 1997. Watershed-based segmentation of 3D MR data for volume quantization. *Magn. Reson. Imag.* 15:679–88
95. Priebe CE, Marchette DJ, Rogers GW. 1997. Segmentation of random fields via borrowed strength density estimation. *IEEE Trans. Pattern Anal. Mach. Intell.* 19:494–99
96. Fosgate CH, Krim H, Irving WW, Karl WC, Willsky AS. 1997. Multiscale segmentation and anomaly enhancement of SAR imagery. *IEEE Trans. Image Process.* 6:7–20

Annual Review of Biomedical Engineering
Volume 2, 2000

CONTENTS